Asian Pub. Corp.

www.asianpubs.org

ARTICLE

Screening of Kabasura Kudineer Chooranam against COVID-19 through Targeting of Main Protease and RNA-Dependent RNA Polymerase of SARS-CoV-2 by Molecular Docking Studies

K. Gopalasatheeskumar[1,✉], Karthikeyen Lakshmanan[2], Anguraj Moulishankar[2], Jerad Suresh[2], D. Kumuthaveni Babu[2] and V.K. Kalaichelvan[1]

Asian Journal of Organic & Medicinal Chemistry

Volume: 5 Year: 2020
Issue: 4 Month: October–December
pp: 319–331
DOI: https://doi.org/10.14233/ajomc.2020.AJOMC-P299

Received: 19 November 2020
Accepted: 5 December 2020
Published: 31 December 2020

ABSTRACT

COVID-19 is the infectious pandemic disease caused by the novel coronavirus. The COVID-19 is spread globally in a short span of time. The Ministry of AYUSH, India which promotes Siddha and other Indian system of medicine recommends the use of formulation like Nilavembu Kudineer and Kaba Sura Kudineer Chooranam (KSKC). The present work seeks to provide the evidence for the action of 74 different constituents of the KSKC formulation acting on two critical targets. That is main protease and SARS-CoV-2 RNA-dependent RNA polymerase target through molecular docking studies. The molecular docking was done by using AutoDock Tools 1.5.6 of the 74 compounds, about 50 compounds yielded docking results against COVID-19 main protease while 42 compounds yielded against SARS-CoV-2 RNA-dependent RNA polymerase. This research has concluded that the KSKC has the lead molecules that inhibits COVID-19's target of main protease of COVID-19 and SARS-CoV-2 RNA-dependent RNA polymerase.

KEYWORDS

SARS-CoV-2, AYUSH, Computational model, AutoDock, *in silico*, Siddha.

INTRODUCTION

Novel coronavirus disease (COVID-19) is the communicable illness caused by the newly exposed coronavirus. This new virus and disease were previously unknown before the occurrence began in Wuhan, China, in December 2019. The older people with comorbidity such as diabetes, cardiovascular disease, chronic respiratory disease and cancer were found to be more vulnerable to this of COVID-19 [1]. On 11th March 2020, WHO has declared COVID-19 outbreak as a pandemic. It has asked nations to take instant action regarding treatment, detection and reduction of transmission immediately. According to the WHO reports on COVID-19 on 25th December 2020, the prevalence of COVID-19 is about 78,761,128 people and 1,710,011 deaths globally. As of 22 April 2020, according to the Ministry of Health & Family Welfare, a total of 465,478

Author affiliations:

[1]Pharmacology Laboratory, Department of Pharmacy, Annamalai University, Annamalai Nagar, Chidambaram-608002, India
[2]Department of Pharmaceutical Chemistry, College of Pharmacy, Madras Medical College, Chennai-600003, India

✉To whom correspondence to be addressed:

E-mail: gskpungai@gmail.com

Available online at: http://ajomc.asianpubs.org

COVID-19 cases, (including 77 foreign nationals) have been reported in 32 states/union territories in India [2]. The COVID-19 virus first spread through droplets of saliva when a diseased person coughs or sneezes. Still date there is no vaccine or particular specific antiviral drugs for the prevention or treatment of COVID-2019. The Indian Council of Medical Research (ICMR), under the Ministry of Health and Family Welfare, has recommended chemoprophylaxis with hydroxychloroquine (400 mg twice on day 1, then 400 mg once a week thereafter) for treating patients with doubted or established COVID-19 patients for healthcare [3,4]. Also the Siddha system of Indian medicine indicates management of COVID-19 like infections by using of Siddha formulations like Nilavembu Kudineer, Kaba Sura Kudineer Chooranam (KSKC) (decoction 60 mL twice a day) and Adathodai Manapagu (syrup 10 mL twice a day) [5]. However, the scientific evidence is not yet reported [6,7]. There are no scientific reports use of the Siddha formulations like Nilavembu Kudineer and KSKC against COVID-19. However toxicity, anti-inflammatory, antipyretic, antibacterial and antioxidant activities of KSKC have been scientifically reported [8]. The KSKC consists of 15 different medicinal plants. It is difficult to screen all the 15 plants against COVID-19. Therefore, the 74 different constituents present in this composition were individually docked against two critical targets of COVID-19 *viz*. SARS-CoV-2 RNA-dependent RNA polymerase (RdRp) and COVID-19 main protease (CVMP) using molecular docking studies.

EXPERIMENTAL

The ability of the drug to reach the site of action is determined by the Lipinski's rule. Molecular docking studies will give us an idea about whether the drug will bind itself to the receptor. This is done by using Autodock tools 1.5.6. The 3D structure of target protein retrived from Protein Data Bank (https://www.rcsb.org) the ligand was downloaded from PubChem database (https://pubchem.ncbi.nlm.nih.gov). The ligand structures were energy minimized in Chem3D Ultra software using MM2 force field. Molecular docking experiments were performed using AutoDock 4 and docking complexes were visualized in 3D by PyMol 2.3 tool and 2D in Molegro molecular viewer 2.5.

Lipinski's rule: Those rules were explaining "the Rule of 5" and also used to determine the ability of the drug to reach the site of action. ADME (adsorption, distribution, metabolism and excretion) properties were predicted by Swiss ADME software freely available in online [9]. In which, As per Lipinski rule molecular weight should be less than 500 DA, Hydrogen Bond donor should be less than or equivalent to 5, Hydrogen bond Acceptor should be less than or equivalent to 10. The list of Lipinski's rule of five of KSKC is shown in Table-1. According to this rule, the compound should not possess more than one violation of this rule. Applications of Lipinski's rule revealed that 42 compounds didn't have any violation, while 22 compounds shows one violation and 12 compounds shows more than one violation. Of the 74 compounds were screened by according to this rule only few of compounds (12 compounds) has more than one violation in KSKC, about 42 compounds possess no violations and 22 compounds produce only one violation, it confirms the most of the active principles in KSKC are orally active drugs.

Retrieval of target protein structure: Three-dimensional crystal structure of RdRp in complex with cofactors (PDB ID: 6M71) with resolution of 2.90 Å was downloaded. This protein structure was determined by electron microscopic method. The

TABLE-1
LIPINSKI'S RULE OF FIVE ON KABASURA KUDINEER CHOORANAM CONSTITUENTS

S. No.	Name	m.w. (Da)	D-HB	A-HB	log P o/w	Violations
1	1,2-Dihydroxy-6,8-dimethoxyxanthone	288.256	1	4.5	2.109	0
2	1,8-Dihydroxy-3,7-dimethoxyxanthone	288.256	0	3.5	2.504	0
3	1-Heptacosanol	396.739	1	1.7	9.461	1
4	2-Phenyl ethylamine	121.182	2	1.57	1.000	1
5	3,7,8-Trimethoxy-1- hydroxyxanthone	300.310	0	4.75	3.082	0
6	4,8-Dihydroxy-2,7-dimethoxyxanthone	288.256	1	4.5	1.998	0
7	7,8-Dimeglucopyrano syloxyflavone	476.436	5	14	0.227	1
8	α-Cyperone	218.338	0	2	3.430	0
9	Anacyclin	271.402	1	2.5	5.298	1
10	Bisabolene	204.355	0	0	6.165	1
11	Berberine	336.360	0	4	2.530	1
12	Chavibetol	164.204	1	1.5	2.675	0
13	Chromin	390.389	1	6.25	3.252	0
14	Copadiene	206.370	0	0	6.886	1
15	Camphene	136.236	0	0	3.237	0
16	Chebulagic acid	954.672	13	26.15	-3.861	3
17	Chebulinic acid	956.688	13	26.15	-3.319	3
18	Clerodane-6-7-dione	722.950	0	9	5.200	33
19	Cryptolepine	232.284	0	2	3.614	0
20	Cyperene	204.355	0	0	4.789	0
21	Cyperol	220.354	1	1.7	3.386	0
22	Cyperolone	236.353	0	2.7	3.167	0
23	Cyperotundone	218.338	0	2	3.090	0
24	Dicatechol sesamine	330.337	4	6.4	1.288	0
25	Dioscin	869.054	8	25.3	1.204	3

26	Diosgenin	414.627	1	3.2	5.932	1
27	Ellagic acid	302.197	4	8	-1.339	0
28	Ephedrine	165.235	2	3.2	1.184	0
29	Ethyl gallate	198.175	3	4.25	0.184	0
30	Eugenol	164.204	1	1.5	2.662	0
31	Furanolactone	470.518	0	11.25	0.906	0
32	Furostanol	402.659	1	3.4	6.179	1
33	Gallic acid	188.130	5	6	0.110	1
34	Gracillin	885.054	9	27	0.321	3
35	Humulene	204.355	0	0	4.873	0
36	Linalol oxide furanoid B	170.251	1	1.5	2.711	0
37	Lupeol	426.724	1	1.7	7.081	1
38	Magnoflorine	342.410	2	4	1.150	0
39	Methyl 3,4,5-trimethoxycinnamate	252.266	0	4.25	2.594	0
40	Methyl gallate	184.148	3	4.25	-0.185	0
41	α-Muurolene	204.355	0	0	5.546	1
42	Pentagalloyl glucose	940.688	15	22.95	-2.948	3
43	Phenyl β-D-glucopyranoside	256.255	4	9.25	-0.329	0
44	Piperine	285.342	0	4.5	3.261	0
45	Piperlongumine	317.341	0	5.25	3.153	0
46	Piperlonguminine	273.331	1	4	3.488	0
47	Plastoquinone	204.268	0	4	1.932	0
48	Prosapogenin A	722.912	6	18.5	2.477	3
49	Quercetin	302.240	4	5.25	0.380	0
50	Rotundenol	222.370	1	1.7	3.465	0
51	Rotundone	218.338	0	2	3.573	0
52	Rutin	610.524	9	20.55	-2.315	3
53	Sugeonol	234.338	1	3.7	2.234	0
54	Tinosporaside	494.538	4	15.7	-0.280	0
55	Tinosporin A	406.432	2	9	1.692	0
56	Vasicine	188.229	1	3.2	1.898	0
57	Zerumbone	218.338	0	2	3.320	0
58	Zingiberene	204.355	0	0	6.307	1
59	α-Curcumene	202.339	0	0	6.247	1
60	α-Farnesene	204.355	0	0	7.030	1
61	α-Tocopherolquinone	446.712	1	4.75	7.434	1
62	Andrographolide	350.454	3	8.1	1.726	0
63	β-Amyrin	426.724	1	1.7	7.040	1
64	β-Bisabolene	204.355	0	0	6.054	1
65	β-Caryophyllene	204.355	0	0	5.054	1
66	β-Selinene	204.355	0	0	5.113	1
67	β-Sesquiphellandrene	204.355	0	0	6.257	1
68	β-Sitosterol	414.713	1	1.7	7.517	1
69	Carotene	536.882	0	0	16.621	2
70	Costusosides	238.369	0	3	3.032	0
71	Inulin	586.720	3	9	3.020	2
72	Pellitorine	223.358	1	2.5	4.078	0
73	Sesamine	354.359	0	6.4	1.763	0
74	Tinosporide	374.390	1	9.25	0.930	0

Molecular weight (m.w.), donor hydrogen bonding (D-HB), acceptor hydrogen bonding (A-HB) log p (octanol-water) values of 74 phytoconstituents of Kabasura Kudineer Chooranam are mentioned and based on the Lipinski's rule of five violations were calculated.

crystal structure of CVMP in complex with an inhibitor N3 (PDB ID: 6LU7), with the resolution of 2.16 Å was downloaded. This protein structure was determined by X-ray diffraction method.

Ligand retrieval and energy minimization: The KSKC consist of 15 medicinal plants such as *Andrographis paniculata* [10], *Clerodendrun serratum* [11], *Zingiber officinale* [12], *Piper longum*, *Syzygium aromaticum* [13], *Justicia beddomei* [14], *Tragia involucrate* [15], *Tinosporia cordifolia* [16], *Anisochilus carnosus* [17], *Cyperus rotundus* [18], *Costus speciosus* [19], *Anacyclus pyrethrum* [20], *Sida acuta* [21], *Hygrophilla auriculata* [22] and *Terminalia chebula* [23]. The active phytochemicals present in these medicinal plants were selected for the ligands (74 compounds) (Table-1). The specified 3D structure of the ligands in sdf.format was imported in Chem3D Ultra and energy minimization was performed using MM2 force field to obtain energetically stable conformation with the least steric strain and saved in PDB format for further use in AutoDock Tools 1.5.6.

Protein and ligand preparation

Protein: The water molecules, cofactors and other ligands were removed from COVID-19 main protease (6LU7) and SARS-CoV-2 RNA-dependent RNA polymerase target (6M71)

through Molegro molecular viewer. Then they were used for molecular docking studies using AutoDock Tools 1.5.6. The Kollaman charges, polar hydrogen were added and charged protein molecule was saved in pdbqt format.

Ligand: The ligand were assigned gasteiger charges and required torsional information and saved in pdbqt format.

Molecular docking studies: The AutoGrid4 module was used to create a grid box of required dimension in Å units along with the direction, with a spacing of 1.0 Å in the protein to create a gpf file. Similarly gpf file was created for the ligand. Then autogrid4 was run to generate Grid maps with the help of a gpf file. The AutoDock4 software ranks the pose based on binding energy difference, unbound and bound conformation. In which docking score are based on the binding affinity between the ligand and protein. The higher negative value of the target known for this potency. The conformational pose of best scores possessing the least energy in the best possible for molecule. The conformations were selected based on the empirical force field and the Lamarackian Genetic Algorithm. The binding affinity between the ligand and protein was pursued by considering the hydrogen bond (intermolecular) interaction and hydrophobic interactions, which were observed between the amino acid residues with the functional group of the small molecules [24].

RESULTS AND DISCUSSION

SARS-CoV-2 is an encased, constructive-sense, single-stranded RNA virus like SARS (severe acute respiratory syndrome) and MERS (middle east respiratory syndrome) coronavirus [25,26]. These viruses have many targets of non-structural proteins such as CVMP, 3-chymotrypsin-like protease, papain-like protease, helicase and RdRp. Of these RdRp and CVMP are two important targets for the replication of RNA viruses like COVOD-19. Many anti-viral drugs have been developed based on these targets for treating infectious diseases such as Hepatitis C, zika and other coronaviruses [27-29]. In the docking study was carried out for the enzymes RdRp and CVMP. Of the 74 compounds that were docked, 50 compounds produced docking results against CVMP while 42 compounds yielded against SARS-CoV-2 RNA-dependent RNA polymerase (Tables 2 and 3). For the CVMP target 9 compounds (β-amyrin, furanolactone, sesa-mine, berberine, clerodane-6,7-dione, lupeol, piperlongumine, piperine and β-sitosterol) have docking score more than -7 kcal/mol. Then 19 compounds have docking score between -5 kcal/mol to -7 kcal/mol. For the RNA dependent RNA polymerase taget 9 compounds (β-sitosterol, piperine, lupeol, sesamine, β-amyrin, piperlongumine, furanolactone, clerodanedione and berberine) have docking score more than

TABLE-2
MOLECULAR DOCKING OF KABASURA KUDINEER CHOORANAM CONSTITUENTS WITH COVID-19 MAIN PROTEASE

S. No.	Compound	2D structure	Binding energy (Kcal/mol)	Ligand efficiency	Inhibit constant (μM)	Internal energy	VDW H-Bond desolvation energy
1	Heptacosanol	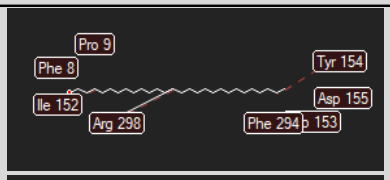	-1.82	-0.07	0.00	-5.94	-5.94
2	Sesamin	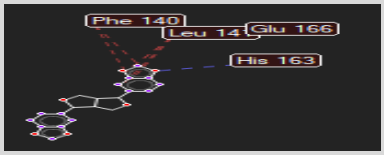	-8.7	-0.33	417.63	-9.3	-0.3
3	Phenethylamine	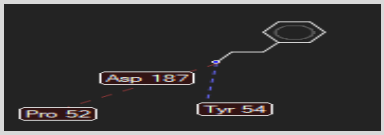	-3.95	-0.44	1.27	-4.85	-4.85
4	α-Farnesene	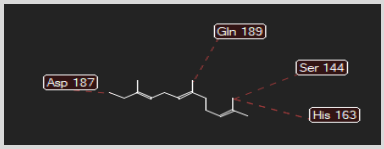	-4.95	-0.35	389	-6.44	-6.44
5	Bisabolene	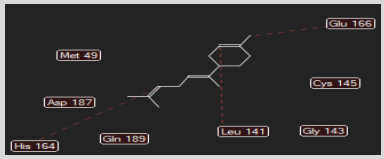	-5.92	-0.39	45.93	-6.81	-6.81
6	Chromine	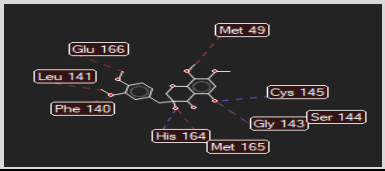	-6.85	-0.29	9.55	-9.23	-9.23

7	α-Curcumene	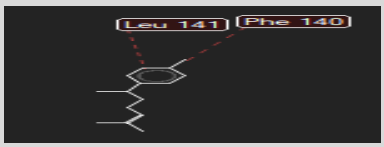	-4.99	-0.33	218.76	-6.19	-6.19
8	Chavibetol		-4.99	-0.37	616.81	-5.57	-5.57
9	Rotundenol	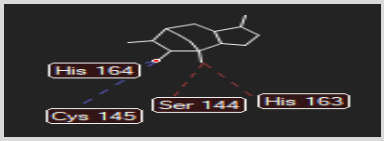	-5.7	-0.36	66.81	-5.99	-5.99
10	Copadien	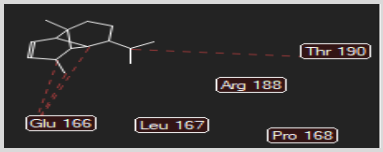	-5.0	-0.33	217.11	-5.3	-5.3
11	β-Sitosterol	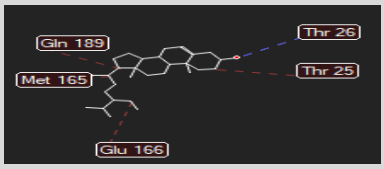	-7.64	-0.25	2.52	-9.72	-9.72
12	Anacyclin	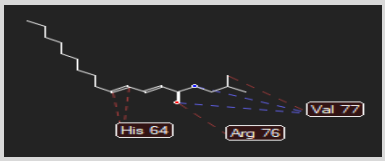	-5.06	-0.25	195.27	-8.04	-8.04
13	Andrographolide	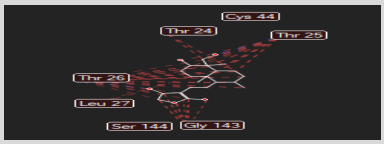	-4.52	-0.18	482.52	-6.61	-6.61
14	Apigenin7glucuronide	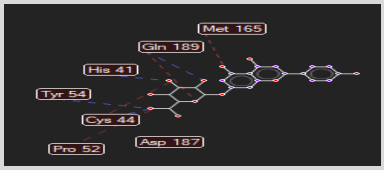	-6.51	-0.2	1.7	-9.19	-9.19
15	Berberine	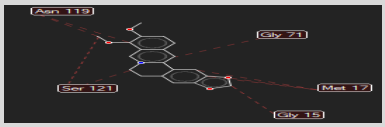	-6.94	-0.28	8.16	-7.54	-7.54
16	β-Amyrin	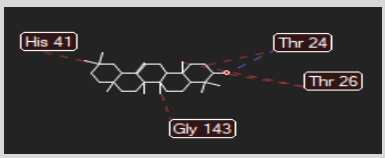	-8.1	-0.26	8.16	-7.54	-7.54
17	β-Bisabolene	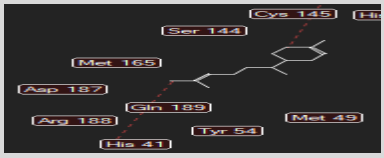	-5.25	-0.26	1.15	-8.4	-8.4
18	β-Caryophyllene		-5.63	-0.38	74.63	-5.63	-5.63

19	β-Selinene	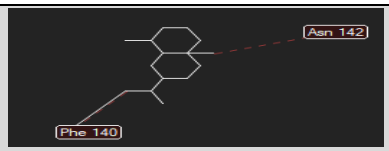	-5.76	-0.38	59.84	-6.06	-6.06
20	Camphene	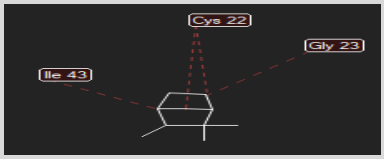	-3.75	-0.38	1.78	-3.75	-3.75
21	Clerodane-6,7-dione	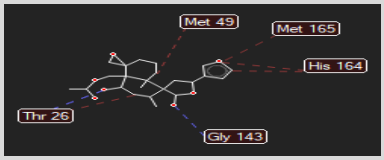	-6.93	-0.23	8.25	-9.32	-9.32
22	Costusosides	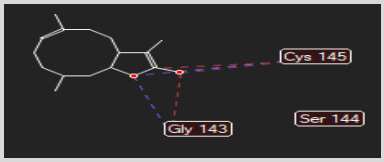	-6.92	-0.41	8.4	-6.92	-6.92
23	Cryptolepine		-6.98	-0.39	7.67	-6.98	-6.98
24	Cyperene	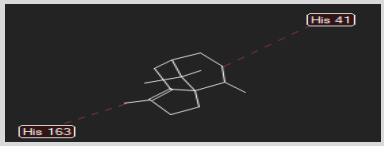	-5.02	-0.33	210.43	-5.02	-5.02
25	Cyperolone	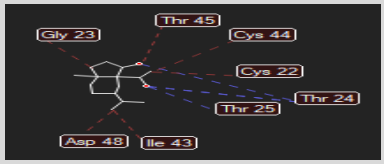	-5.34	-0.31	210.43	-5.02	-5.02
26	Cyperotundone	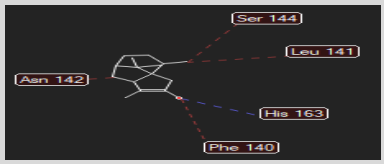	-6.87	-0.43	9.15	-6.87	-6.87
27	Dioscin	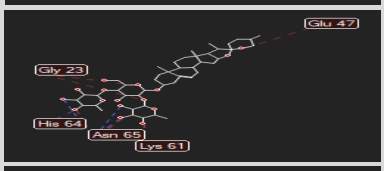	-4.99	-0.08	218.88	-9.47	-9.47
28	Diosgenin	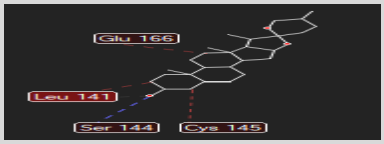	-9.43	-0.32	114.24	-9.72	-9.72
29	Eugenol	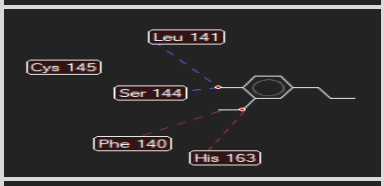	-5.3	-0.44	131.02	-6.49	-6.49
30	Furanolactone	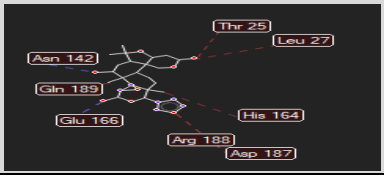	-9.82	-0.29	63.24	-10.12	-10.12

31	Furostanol	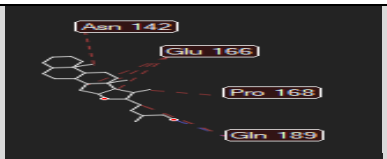	-8.23	-0.28	929.26	-9.15	-9.15
32	Gracillin	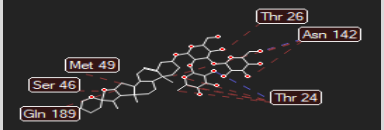	-3.3	-0.05	3.79	-8.38	-8.38
33	Lupeol		-8.55	-0.28	539.74	-9.15	-9.15
34	Magnoflorine	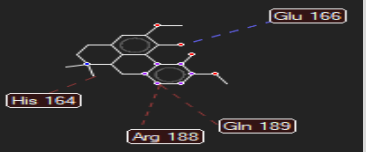	-9.35	-0.37	14.09	-10.54	-10.94
35	Pellitorine	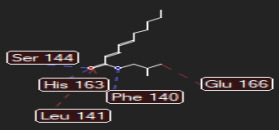	-5.41	-0.34	108.72	-7.79	-7.79
36	Pentagalloylglucose	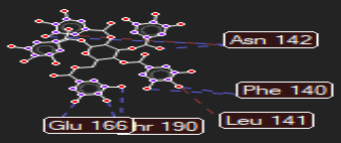	-3.83	-0.06	5.41	-5.16	-5.16
37	Piperine	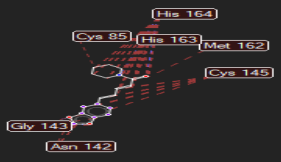	-5.65	-0.27	72.6	-6.54	-6.54
38	Piperlongumine	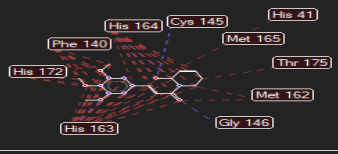	-7.44	-0.32	3.53	-8.93	-8.93
39	Piperlonguminine	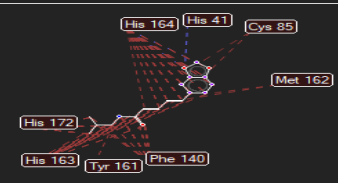	-7.79	-0.4	1.43	-9.46	-9.46
40	Plastoquinone	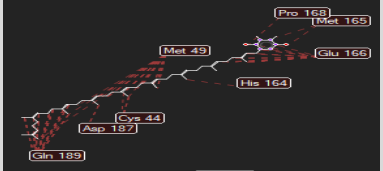	-0.58	-0.01	373.85	-8.34	-8.34
41	Quercetin		-7.77	-0.35	2.02	-9.56	-9.56
42	Rotundone	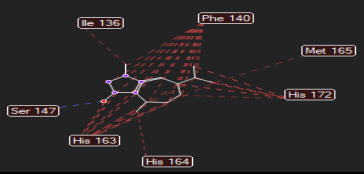	-5.64	-0.35	73.23	-5.94	-5.94

43	Rutin	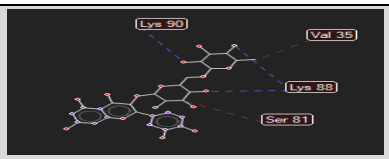	-3.53	-0.08	2.59	-8.3	-8.3
44	Sugeonol	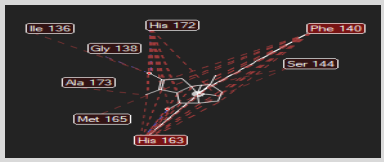	-5.79	-0.34	57.45	-6.08	-6.08
45	Tinosporaside	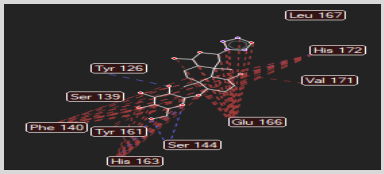	-6.28	-0.18	24.95	-8.67	-8.67
46	Tinosporide		-7.45	-0.28	3.45	-8.05	-8.05
47	Vasicine	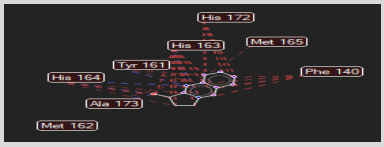	-5.81	-0.42	55.37	-6.11	-6.11
48	Zerumbone		-6.3	-0.39	24	-6.3	-6.3
49	Zingiberene		-4.41	-0.29	583.3	-5.6	-5.6
50	Humulene		-5.99	-0.4	40.98	-5.99	-5.99

2D structure of compounds in COVID-19 main protease the blue line denotes the amino acid interaction of hydrogen bonding and the red line denotes the static interaction. Binding energy, Ligand efficiency, Inhibit constant, Internal energy and VDW H-Bond desolvation energy were obtained from AutoDock 4.

TABLE-3
MOLECULAR DOCKING OF KABASURA KUDINEER CHOORANAM CONSTITUENTS WITH RNA-DEPENDENT RNA POLYMERASE OF SARS-CoV-2

S. No.	Compound	2D structure	Binding energy (Kcal/mol)	Ligand efficiency	Inhibit constant (μM)	Internal energy	VDW H-Bond desolvation energy
1	α-Cyperone	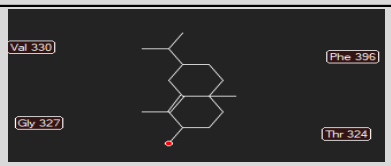	-6.72	-0.42	11.94	-7.01	-7.01
2	α-Curcumene	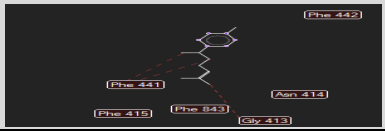	-4.15	-0.24	311.35	-8.22	-8.22

3	Anacyclin	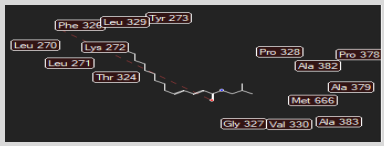	-4.78	-0.24	311.35	-7.77	-7.77
4	Andrographolide	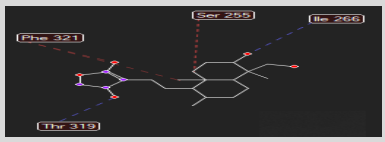	-6.13	-0.25	32.17	-8.22	-8.22
5	Berberine	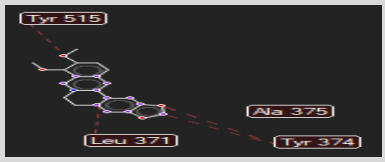	-7.56	-0.3	2.89	-8.15	-8.15
6	β-Amyrin	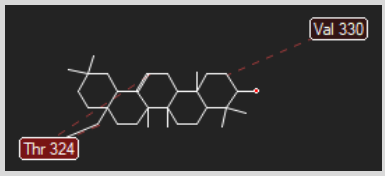	-9.36	-0.3	137.01	-9.66	-.9.66
7	β-Bisabolene	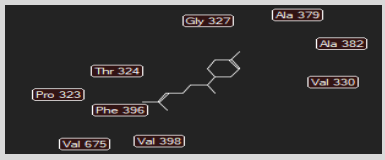	-.4.88	-0.33	263.44	-6.08	-6.08
8	β-Caryophyllene	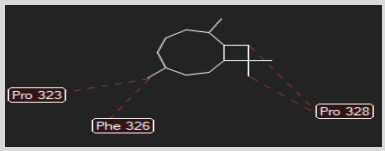	-5.76	-0.38	59.35	-5.76	-5.76
9	β-Selinene	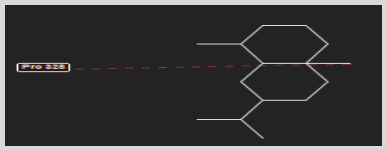	-5.98	-0.4	41.29	-6.28	-6.28
10	Camphene	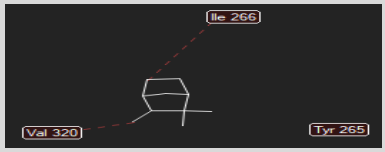	-4.44	-0.44	559.87	-4.44	-4.44
11	Clerodane-6,7-dione	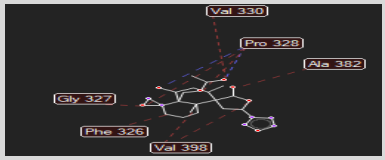	-7.25	-0.24	4.81	-9.64	-9.64
12	Costusosides	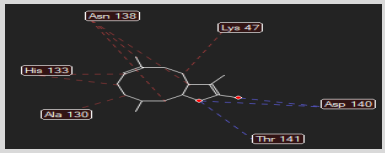	-5.54	-0.33	87.36	-5.54	-5.61
13	Cryptolepine		-5.21	-0.29	151.7	-5.21	-5.21
14	Cyperene	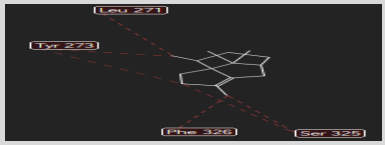	-5.71	-0.38	65.02	-5.71	-5.7

15	Cyperol	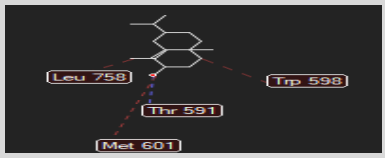	-5.21	-0.36	56.85	-6.39	-6.39
16	Cyperotundone	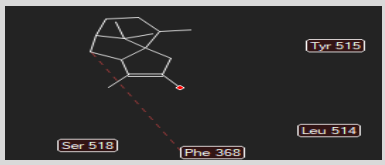	-5.72	-0.36	64.14	-5.72	-5.72
17	Ephedrine		-4.26	-0.36	754.39	-5.45	-5.45
18	Eugenol	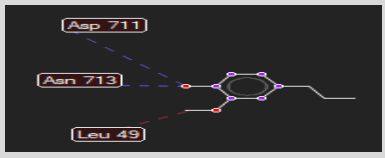	-3.85	-0.32	1.51	-5.04	-5.04
19	Furanolactone		-9.55	-0.28	100.17	-9.85	-9.85
20	Furostanol	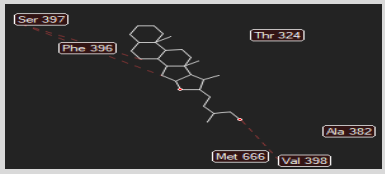	-6.26	-0.22	25.69	-7.75	-7.75
21	Lupeol	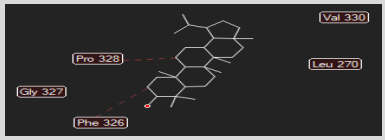	-7.84	-0.25	1.8	-8.43	-8.43
22	Pellitorine		-5.38	-0.34	112.94	-7.77	-7.77
23	Pentagalloylglucose	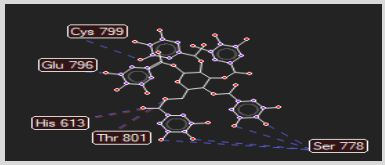	-0.48	-0.01	445.06	-9.73	-9.73
24	Piperine		-7.08	-0.34	6.44	-7.96	-7.96
25	Piperlongumine	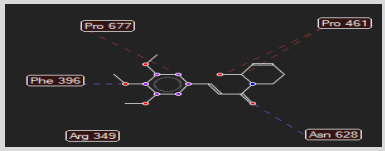	-7.13	-0.31	5.9	-8.63	-8.63
26	Piperlonguminine	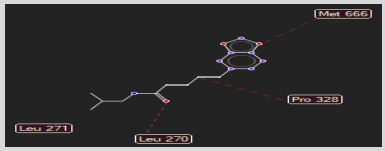	-6.73	-0.31	5.9	-8.63	-8.63

27	Plastoquinone	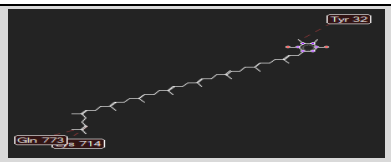	-1.74	-0.03	11.29	-8.63	-8.63
28	Quercetin	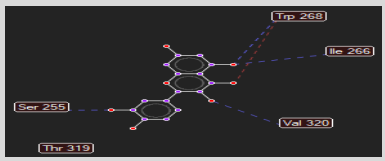	-6.37	-0.029	21.31	-8.16	-8.16
29	Rotundone	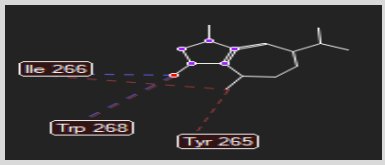	-5.57	-0.35	82.22	-5.87	-5.87
30	Rutin	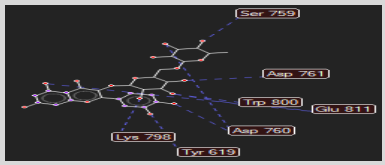	-6.7	-0.16	12.23	-11.47	-11.47
31	Zerumbone		-5.74	-0.36	62.51	-5.74	-5.74
32	Humulene		-5.38	-0.36	114.32	-5.38	-5.38
33	Phenethylamine	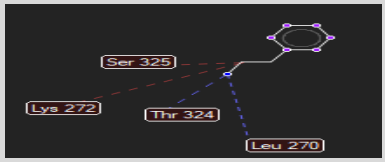	-3.78	-0.42	1.71	-4.62	-4.62
34	Sesamine	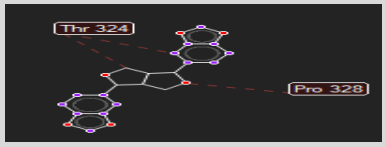	-8.85	-0.34	33.27	-9.45	-9.45
35	Heptacosanol	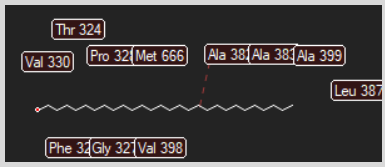	-2.37	-0.08	0.00	-5.39	-5.39
36	β-Sesquiphellandrene	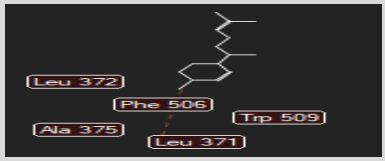	-4.76	-0.32	324.37	-5.95	-5.95
37	α-Farnesene	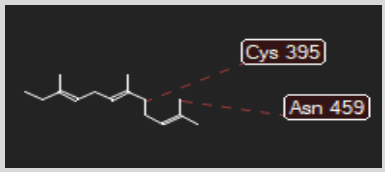	-4.67	-0.31	378.94	-5.95	-5.95
38	β-Sitosterol	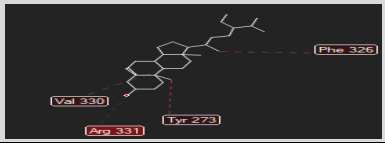	-7.6	-0.25	2.69	-9.69	-9.69

39	Copadiene	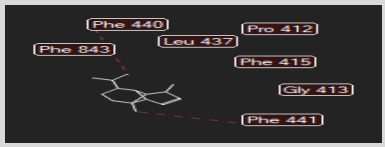	-4.87	-0.32	269.75	-5.17	-5.17
40	Chavibetol	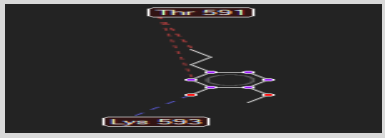	-3.57	-0.3	2.4	-4.77	-4.69
41	3-(3,4-Dimethoxyphenyl) -7,8-dimethoxy-2,3-dihydrochromen-4-one	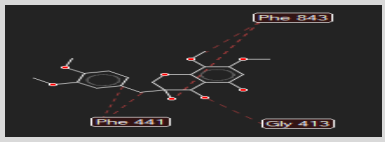	-6.62	-0.24	14.14	-9.0	-9.0
42	β-Bisabolene		-5.91	-0.39	46.68	-6.8	-6.8

2D structure of compounds in RNA-dependent RNA polymerase of SARS-CoV-2 the blue line denotes the amino acid interaction of hydrogen bonding and the red line denotes the static interaction. Binding energy, Ligand efficiency, Inhibit constant, Internal energy and VDW H-Bond desolvation energy were obtained from AutoDock 4.

-7 kcal/mol. Then 19 compounds have docking score between -5 kcal/mol to -7 kcal/mol. The active sites amino acids which are responsible for good interaction through hydrogen bonding. In which eugenol, pellitorin and pentagalloyl glucose were revealed the high hydrogen boding to the target of CVMP.

In case of the eugenol hydrogen bond interaction with SER144 and LEU141 amino acid shows interaction. In the case of pellitorin hydrogen bond interaction with SER144, HIS163 and PHE140 amino acid shows interaction. The case of pentagalloyl glucose hydrogen bond interaction with SER144, HIS163 and PHE140 shows interactions. Then andrographolide, rutin and sesamine were revealed the high hydrogen boding to the target of RdRp. In the case of andrographolide hydrogen bond interaction with THR318 amino acid shows the interaction. In the case of sesamine hydrogen bond interaction with VAL330 amino acid shows the interaction. In the case of rutin hydrogen bond interaction with SER759, ASP761, TRP800, GLU811, ASP760, TYR619 and LYS798 amino acid shows the interaction. In the cases of sesamine hydrogen bond interaction VAL330 amino acid shows the interaction.

The traditional use of KSKC is reported to have a good antiviral activity. The current work justifies the constituents in this KSKC bind well with the critical target main protease of COVID-19 and SARS-CoV-2 RNA-dependent RNA polymerase and it may be possible to use in the treatment of COVID-19.

Conclusion

in silico results of this research work concluded that, many of the active constituent of the KSKC shows the good affinity with the main protease and RdRp. The active constituents can be taken as lead molecules and further developed to produce a drug candidate for COVID-19. The further enzyme based inhibitory study (*in vitro*) needs to conduct to confirm these results.

REFERENCES

1. A. Moulishankar, M. Ramasamy, S. Ravichandran and G. Kasiramar, Review on COVID-19, *Asian J. Res. Pharm. Sci. Biotechnol.*, **8**, 72 (2020).
2. WHO reports Coronavirus Disease (COVID-19) (2020); https://covid19.who.int/
3. S. Rathi, I. Pranav, K. Ashwini and K. Shriprakash, Hydroxychloroquine Prophylaxis for COVID-19 Contacts in India, *Lancet Infect. Dis.*, **20**, 1118 (2020); https://doi.org/10.1016/S1473-3099(20)30313-3
4. National Taskforce for COVID-19 Advisory on the Use of Hydroxychloroquine as Prophylaxis for SARS-CoV-2 infection (2020).
5. Advisory from Ministry of AYUSH for Meeting the Challenge Arising Out of Spread of Coronavirus (Covid-19) in India dated 6th March 2020.
6. A.K. Singh, A. Singh, A. Shaikh, R. Singh and A. Misra, Chloroquine and Hydroxychloroquine in the Treatment of Covid-19 with or without Diabetes: A Systematic Search and a Narrative Review with a Special Reference to India and other Developing Countries, *Diabetes Metab. Syndr.*, **14**, 241 (2020); https://doi.org/10.1016/j.dsx.2020.03.011
7. P. Gautret, J.C. Lagier, P. Parola, V.T. Hoang, L. Meddeb, M. Mailhe, B. Doudier, J. Courjon, V. Giordanengo, V.E. Vieira, H. Tissot Dupont, S. Honoré, P. Colson, E. Chabrière, B. La Scola, J.-M. Rolain, P. Brouqui and D. Raoult, Hydroxychloroquine and Azithromycin as a Treatment of Covid-19: Results of an Open-label Non-Randomized Clinical Trial, *Int. J. Antimicrob. Agents*, **56**, 105949 (2020); https://doi.org/10.1016/j.ijantimicag.2020.105949
8. J. Saravanan, D. Neethu, K. Gopalasatheeskumar, V. Sanish Devan, K. Thanga Kokila and M. Sanjay, Anti-inflammatory, Antipyretic and Antibacterial Study of Kabasura Kudineer Choornam, *Int. J. Curr. Adv. Res.*, **7**, 9992 (2018); https://doi.org/10.24327/ijcar.2018.9997.1672
9. C.A. Lipinski, F. Lombardo, B.W. Dominy and P.J. Feeney, Experimental and Computational Approaches to Estimate Solubility and Permeability in Drug Discovery and Development Settings, *Adv. Drug Deliv. Rev.*, **46**, 3 (2001); https://doi.org/10.1016/S0169-409X(00)00129-0
10. M.S. Hossain, Z. Urbi, A. Sule and K.M. Hafizur Rahman, *Andrographis paniculata* (Burm. f.) Wall. ex Nees: A Review of Ethnobotany, Phytochemistry and Pharmacology, *Scientific World J.*, **27**, 4905 (2014); https://doi.org/10.1155/2014/274905
11. J.J. Patel, S.R. Acharya and N.S. Acharya, *Clerodendrum serratum* (L.) Moon.-A Review on Traditional Uses, Phytochemistry and Pharmacological Activities, *J. Ethnopharmacol.*, **154**, 268 (2014); https://doi.org/10.1016/j.jep.2014.03.071

12. Q.Q. Mao, X.Y. Xu, S.Y. Cao, R.-Y. Gan, H. Corke, T. Beta and H.-B. Li, Bioactive Compounds and Bioactivities of Ginger (*Zingiber officinale* Roscoe), *Foods*, **8**, 185 (2019); https://doi.org/10.3390/foods8060185
13. K. Kaur and S. Kaushal,Phytochemistry and Pharmacological Aspects of *Syzygium aromaticum*: A Review, *J. Pharmacogn. Phytochem.*, **8**, 398 (2019).
14. A. Marathakam, N. Kannappan, S. Jasemine, A. Santhiagu, M. Sreejith and M.P. Ajith, Studies on Phytochemical and *in vitro* Antioxidant Potential of *Justicia beddomei* (Clarke) *Bennett*, *Free Rad. Antiox.*, **2**, 26 (2012); https://doi.org/10.5530/ax.2012.4.5
15. P. Ravi, V. RamaRao, K.E. Pravallika, Phytochemical, Pharmacological Profiles of *Tragia involucrate*, *Int. J. Chemtech Res.*, **11**, 37 (2018).
16. P. Sharma, B.P. Dwivedee, D. Bisht, A.K. Dash and D. Kumar, The Chemical Constituents and Diverse Pharmacological Importance of *Tinospora cordifolia*, *Heliyon*, **5**, e02437 (2019); https://doi.org/10.1016/j.heliyon.2019.e02437
17. P.R. Sardar, S.R. Manik, Therapeutic Potential of Aromatic Phyto-constituents Derived from *Anisochilus carnosus* (L.) Wall, *Int. J. Appl. Res*., **3(3S)**, 194 (2017).
18. A.M. Peerzada, H.H. Ali, M. Naeem, M. Latif, A.H. Bukhari and A. Tanveer, *Cyperus rotundus* L.: Traditional Uses, Phytochemistry and Pharmacological Activities, *J. Ethnopharmacol.*, **174**, 540 (2015); https://doi.org/10.1016/j.jep.2015.08.012
19. A.H. El-Far, H.M. Shaheen, A.W. Alsenosy, Y.S. El-Sayed, S.K. Al Jaouni and S.A. Mousa, *Costus speciosus*: Traditional Uses, Phytochemistry, and Therapeutic Potentials, *Phcog. Rev.*, **12**, 120 (2018); https://doi.org/10.4103/phrev.phrev_29_17
20. A. Usmani, M. Khushtar, M. Arif, M. Siddiqui, S. Singh and M. Mujahid, Pharmacognostic and Phytopharmacology Study of *Anacyclus pyrethrum*: An Insight, *J. Appl. Pharm. Sci.*, **6**, 144 (2016); https://doi.org/10.7324/JAPS.2016.60325
21. F. Jose, S. Lal, S. Lekshmi, V. Jiju and E. Abraham, Purified Water from Urine: A Review, *Pharma. Innovation*, **6**, 1 (2017); https://doi.org/10.7897/2277-4572.06142
22. A.D. Kshirsagar, K.G. Ingale, N.S. Vyawahare and V.S. Thorve, *Hygrophila spinosa*: A Comprehensive Review, *Pharmacogn. Rev.*, **4**, 167 (2010); https://doi.org/10.4103/0973-7847.70912
23. Promila and V.K. Madan, Therapeutic & Phytochemical Profiling of *Terminalia chebula* Retz. (Harad): A Review, *J. Med. Plants Stud.*, **6**, 25 (2018).
24. A. Moulishankar and K. Lakshmanan, Data on Molecular Docking of Naturally Occurring Flavonoids with Biologically Important Targets, *Data Brief*, **29**, 105243 (2020); https://doi.org/10.1016/j.dib.2020.105243
25. M. Pal, G. Berhanu, C. Desalegn and V. Kandi, Severe Acute Respiratory Syndrome Coronavirus-2 (SARS-CoV-2): An Update, *Cureus*, **12**, 7423 (2020); https://doi.org/10.7759/cureus.7423
26. A. Zumla, J.F.W. Chan, E.I. Azhar, D.S.C. Hui and K.Y. Yuen, Coronaviruses–Drug Discovery and Therapeutic Options, *Nat. Rev. Drug Discov.*, **15**, 327 (2016); https://doi.org/10.1038/nrd.2015.37
27. A.A. Elfiky, Ribavirin, Remdesivir, Sofosbuvir, Galidesivir, and Tenofovir against SARS-CoV-2 RNA Dependent RNA Polymerase (RdRp): A Molecular Docking Study, *Life Sci.*, **117**, 592 (2020); https://doi.org/10.1016/j.lfs.2020.117592
28. X. Xue, H. Yu, H. Yang, F. Xue, Z. Wu, W. Shen, J. Li, Z. Zhou, Y. Ding, Q. Zhao, X.C. Zhang, M. Liao, M. Bartlam and Z. Rao, Structures of Two Coronavirus Main Proteases: Implications for Substrate Binding and Antiviral Drug Design, *J. Virol.*, **82**, 2515 (2008); https://doi.org/10.1128/JVI.02114-07
29. D. Sivaraman and P.S. Pradeep, Revealing Anti-viral Potential of Bio-active Therapeutics Targeting SARS-CoV2- polymerase (RdRp) in Combating COVID-19: Molecular Investigation on Indian Traditional Medicines, *Preprints*, **2020**, 2020030450 (2020); https://doi.org/10.20944/preprints202003.0450.v1